

BUNCH RESOLVED TRANSVERSE BEAM DIAGNOSTICS AT BESSY II*

I. Shmidt[†], G. Rehm, G. Schiawietz

Helmholtz-Zentrum Berlin für Materialien und Energie, Berlin, Germany

Abstract

For diagnostics of the different bunch types at the BESSY II electron-storage ring, a streak camera and a fast-gated ICCD camera have been installed at two neighbouring beam-lines, both of which are powered by visible light from the same dipole magnet. This contribution is focused on the ICCD camera and its first applications. After an improvement regarding the ICCD repetition rate, the maximum illumination rate exceeds now the BESSY II revolution frequency of 1.25 MHz. Furthermore, we have improved the optical light-transfer system and characterized the optical magnification, the spatial resolution and time resolution of the system.

Initial measurements have been restricted to direct bunch-resolved imaging of the 2-dimensional transverse shapes of different types of bunches. Specifically, the Pulse Picking by Resonant Excitation (PPRE) bunch is investigated in more detail. This bunch is horizontally broadened by a quasi-resonant incoherent perturbation and leads to pseudo single-bunch radiation within the complex multi-bunch fill-pattern at the BESSY II storage ring.

INTRODUCTION

BESSY II, like other modern synchrotron light sources, has a complex filling pattern in standard user mode. Existence of the special bunches in the ring allows to use the emitted synchrotron radiation for more purposes. Apart from the 'normal' train bunches, that have approx. 1 mA current in each of the bunches BESSY II has also one Camshaft bunch (4 mA) and two PPRE bunches (3 mA each) and seven slicing bunches (3 mA each). Especially the PPRE bunch is of interest for the bunch resolved diagnostics. This bunch makes it possible to run experiments that require pulsed synchrotron radiation with repetition rates in few MHz range in the standard user operation. To achieve that the bunch is excited in the horizontal direction which allows the user to work with the light of the PPRE bunch only just by blocking the light from the other bunches with an aperture [1]. Therefore it is important to broaden the bunch significantly without exciting large center of mass motion. An analytical model as well as numerical simulations on the excitation mechanism of PPRE bunch were already presented in [2]. To get information on the real behavior of the bunch, time consuming life time measurements or operation in the single bunch mode were required previously. However, using a fast-gated ICCD camera allows direct observation of the bunch behavior. In the following, a beamline for bunch resolved

transverse diagnostics using a fast-gated ICCD camera will be described. Additionally, results of the first observations of the PPRE bunch will be presented.

BEAMLINE FOR TRANSVERSE OPTICAL DIAGNOSTICS

Both optical diagnostic beamlines - for longitudinal diagnostics with Streak camera and for transverse diagnostics with fast-gated ICCD - are located in the sector 12 of the BESSY II ring and start from the bending magnet BM2T6R [3]. For transverse diagnostics, synchrotron light is transferred from the storage ring to the diagnostic platform with two custom-made plane 70 mm×70 mm mirrors M1 and M2 with residual bending radii of > 25 km (see Fig. 1). An important part of the beamline is the X-ray blocking baffle that covers 5.31 mm in the center of the light bulk, preventing X-Rays from reaching the first mirror. Apart from the central block, the X-ray blocking baffle also defines with its outer dimensions the acceptance angle of the beamline. It has a horizontal aperture of 44 mm and vertical aperture of 31.3 mm with resulting acceptance angles of 6.10 mrad and 4.34 mrad. The vacuum part of the beamline closes with a combination of two wedged windows, that are 180° rotated relative to each other. This combination allows to avoid multiple reflections between the outlet window and mirror M2 without changing the transmitted part of the light.

At this point it is important to mention that limited acceptance of the beamline as well as the wavelength of the used light limit the spatial resolution of the beamline. According to the Rayleigh criterion, the smallest resolvable angle for the single slit of the width d illuminated with a monochrome light of the wavelength λ is $\theta = \arcsin(\frac{\lambda}{d}) \approx \frac{\lambda}{d}$. Therefore, the smallest resolvable transverse distance of the set up is: spatial resolution at the distance l from the slit, is $b = l \cdot \tan(\theta) \approx l \cdot \frac{\lambda}{d}$. Which in this case results in the smallest resolvable full width at half maximum (FWHM) of the electron beam of about 100 μm in horizontal direction and 140 μm in vertical direction for the green light.

Next, the light is guided on the optical table by three further plain 10 cm×10 cm mirrors M3 - M5 in the direction of the cameras. There are two set-ups available that focus the incoming light into both CCD and fast-gated ICCD. The overview of both optics is shown in Fig. 2. In both cases the final lens is used for additional magnification of the received image. Though for external optics just one main focusing is used. It stays on the optical table and is therefore easy to adjust and remove. In case of internal optics light is getting focused by the lens that is located inside the vacuum chamber between mirrors M1 and M2. This lens can only be moved in one direction: moved in and out of the light path. However its position can't be adjusted. Therefore one more correction

* Work supported by German Bundesministerium für Bildung und Forschung, Land Berlin, and grants of Helmholtz Association

[†] irma.shmidt@helmholtz-berlin.de

Table 1: Locations and Magnification Factors of the Lenses

	f , mm	h_o , mm	h_i , mm	M
in-vacuum lens	3430	7988.5	6009 ± 1	0.7523 ± 0.0001
correction lens	155	145 ± 1	75 ± 1	0.52 ± 0.01
focusing lens on the table	750	13127 ± 1	801 ± 1	0.06101 ± 0.00008
final lens	40	51 ± 1	203 ± 1	3.98 ± 0.09

lens has to be used on the optical table to keep the same intermediate focal point for both optics so that the final lens doesn't have to be moved when changing set-ups.

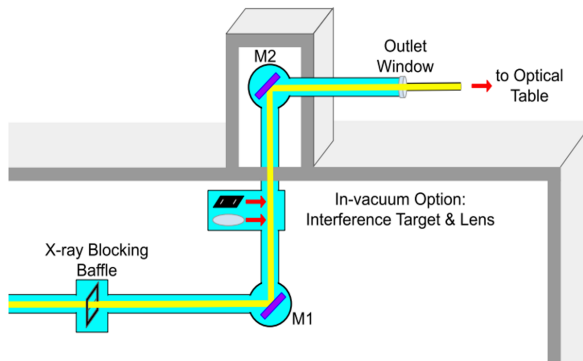


Figure 1: Overview of the in-vacuum part of the beamline for transverse beam diagnostics. Figure taken from [4].

The main difference between the set-ups is its resulting magnification. Knowing the distances between each used lens and its object h_o and image h_i it is possible to calculate the final magnification ($M = \frac{h_i}{h_o}$) of the used set-up of lenses. Measured distances as well as resulting magnifications for each of the used lenses are summarized in the Table 1. Note that all of the lenses are achromatic doublets. Resulting final magnifications of are therefore 1.55 ± 0.07 for internal optics and is 0.24 ± 0.01 for external optics.

After passing the final lens, the light gets divided in two parts by a 50/50 beam splitter. That allows parallel use of the CCD and fast gated ICCD cameras and its comparison. On its way on the optical table light passes also through a polariser, wavelength filter and a neutral density filter. Typically, a neutral density filter with 80 % transmittance, a

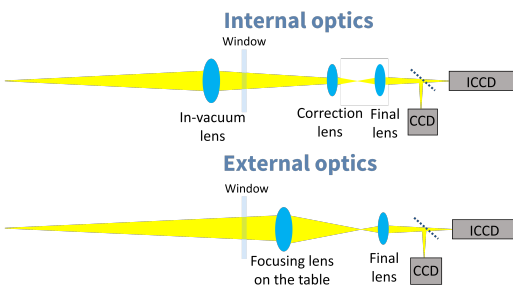


Figure 2: Schematic overview of the two possible set-ups for the transverse beam diagnostics.

550 ± 10 nm wavelength filter and sigma polarisation were chosen.

FAST-GATED ICCD CAMERA

The fast-gated ICCD camera that is used at BESSY II is a *XXRapidFrame* camera from *Stanford Computer Optics* [5]. An important characteristic of the camera is that it consists of four individual intensified cameras (*4Picos-dig*) that are packed together in one housing with just one entrance for the light. Each of four internal cameras inside the fast-gated ICCD deliver images of 1360×1024 pixels with pixel size $4.7 \times 4.7 \mu\text{m}$. To forward light at all the four internal cameras via a pyramid mirror is used (see Fig. 3). Each of the cameras has its own image intensifier (single stage multi channel plate (MCP)). The gating is enabled by manipulating of the power supply of the photo cathode in front of the MCP. This enables the fast and individual gating of all of the four inside cameras, so that all of them can be used in parallel still remaining independent from each other. However this is only possible if parallel light is entering the camera housing. Otherwise, the four cameras show different parts of the initial image, depending on how the light was split by the pyramidal mirror. Therefore, in our case using focused light, it is only possible to use one out of four cameras.

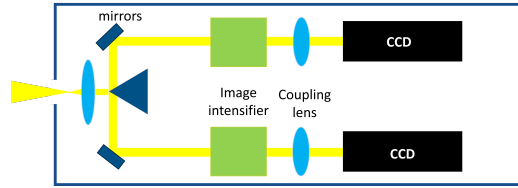


Figure 3: Schema of the set-up inside the fast-gated ICCD (side view).

The fast-gated ICCD camera can be triggered by an external trigger or internally. After the upgrade of the camera, the maximal possible trigger frequency increased from 200 kHz to 1.5 MHz. This change was necessary to be able to follow the revolution frequency of BESSY II (1.25 MHz). However, the increase of the maximal possible trigger frequency influenced the time resolution of the system. Before the upgrade, the shortest possible gating time was about 200 ps. The increase of trigger frequency, was expected to result in a slight deterioration of the gating time. To check the change of the gating time the intensity of the camshaft bunch was measured in dependency of the delay times for three different gating times: 200 ps, 400 ps, and 600 ps. Results of the measurements are shown in the Fig. 4. For all cases real resolution is higher than the chosen gating time. It is interesting to note, that for both 200 ps and 400 ps the measured FWHM of the bunch length is very similar and is about 700 ps, which is significantly larger than the chosen gating times. However, real average bunch sizes at BESSY II are in range of 20 ps [6] with 2 ns distance from each other. Therefore even that increased gating times are suitable for the transverse bunch diagnostics.

The possibility to use ICCD camera with external trigger with up to 1.5 MHz in combination with the shortest exposure times allows to look at individual bunches in individual turns, whereby the choice of bunch in the filling pattern happens by changing the delay time of the camera (time between arrival of the trigger signal and opening of the camera gate). It is also possible to integrate over multiple bunches and/or turns by extending the exposure time or repetitive use of the trigger. For one image it is possible to use the trigger up to 127 times. Therefore, it is possible to integrate the light of the chosen bunch from up to 127 turns. It is important to note that image transfer from the camera to the computer takes much more time than the chosen exposure times, namely about 0.1 s. This means an image can be obtained for a single bunch in a single turn, but it is not possible to see multiple consecutive turns.

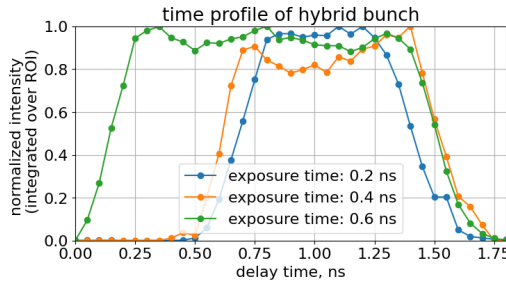


Figure 4: Measurement of the time resolution of the fast-gated ICCD camera.

EXPERIMENTAL PROOF OF MAGNIFICATION FACTOR

To be able to use both fast-gated ICCD and CCD cameras for beam diagnostics it is crucial to know the magnification factor between received image and its actual source. Thereby, it is important to remember, that the camera might also introduce additional magnification to the obtained image. In the CCD camera light is guided directly to the photo-sensitive chip so the image remains unchanged. However, in the fast-gated ICCD camera there are several optical elements that light passes before reaching the final CCD chip. Since both cameras share the set-up on the optical table, it is possible to get the magnification by the ICCD camera through comparison of its image with the simultaneously taken CCD image. The result of the comparison of the beam profiles from both cameras in combination with internal optics is shown in Fig. 5. The difference in distances between main peak and first secondary maxima gives difference in magnification, showing the additional factor of 1.12 for the ICCD. Combining this factor with the magnification of the optics we receive the final magnification of the beamline with ICCD camera of 1.74 ± 0.08 for internal optics and 0.27 ± 0.01 for external optics.

After the individual magnification factors for optical set-ups and the ICCD are known the final magnifications were compared to the experimentally measured values. To that

Table 2: Experimentally Measured Magnifications Factors of the Set-ups

		ICCD	
		Experimental	Optical
Internal optics	horizontal	1.57	1.74 ± 0.08
	vertical	1.51	
External optics	horizontal	0.26	0.27 ± 0.01
	vertical	0.22	
		CCD	
		Experimental	Optical
Internal optics	horizontal	1.32	1.55 ± 0.07
	vertical	1.27	
External optics	horizontal	0.21	0.24 ± 0.01
	vertical	0.18	

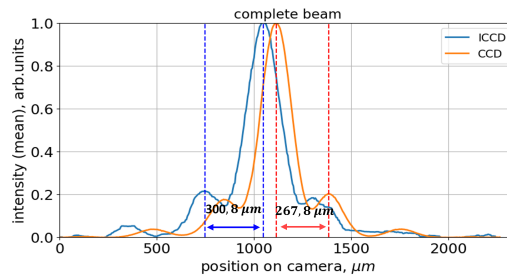


Figure 5: Comparison of the beam profile at ICCD and CCD cameras (Note: ICCD image is vertically mirrored relative to CCD image).

end, the beam was moved by approximately 1 mm with help of corrector magnets first horizontally and then vertically and the change of the beam position in the camera image was detected. This method delivers the magnification factor of the whole set-up: from initial object (beam) to final image on the camera. Resulting values are presented in the Table 2. The discrepancies between optically calculated and experimentally determined magnification factor are assigned to poor calibration factors used in the electron BPMs in BESSY II.

EXAMPLE OF MEASUREMENTS: PPRE BUNCH

After all the important characteristics of the beamline as well as fast-gated ICCD camera are known, the set-up can be used for bunch resolved transverse diagnostics. With the fast-gated ICCD it is possible to receive images of individual bunches, and thus measurements of the PPRE bunch can be done in the standard user operation settings, with the standard filling pattern and standard way to excite the bunch.

Excitation of the PPRE bunch in BESSY II is enabled by the bunch-by-bunch feedback system, which allows to kick individual bunches in the ring. In the standard case, the excitation frequency for PPRE is calculated and applied by a separate DimTel [7] unit and an extra kicker. During the following experiment excitation frequency for the PPRE bunch was approx. 1064.5 kHz. This frequency depends on the betatron frequency [2], which is measured during the operation on one of the train bunches and is then used to adjust excitation frequency of the PPRE bunch to the state

of the machine at each moment. This adjustment happens once every second.

For the following measurements external optics has been used. However to increase intensity of incoming light to take single turn images with the camera the wavelength filter was removed from the set-up.

In Fig. 6, images of not excited and excited state of the single PPRE bunch are shown together with their profiles. It can be seen, that in the excited state the bunch almost doubles its size in horizontal direction. The exact size of the bunch can be obtained for instance by fitting the recorded profiles. Figure 7 shows variation of the bunch size and its relative position in time for both conditions of the PPRE bunch. Notable is that due to the excitation of the bunch its size increases from $241 \pm 4 \mu\text{m}$ to $404 \pm 29 \mu\text{m}$, however it keeps changing in time delivering higher measurement uncertainty for the PPRE users. Also amplitude of the center of mass motion increases significantly: from $10 \mu\text{m}$ rms to $34 \mu\text{m}$, with excitation spikes related to the bunch-size maxima.

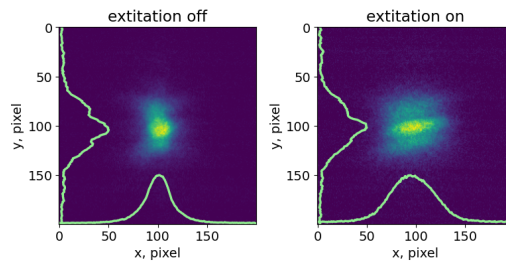


Figure 6: Image of the PPRE bunch in the excited and not excited state.

Another important dependency that is possible to see using fast-gated ICCD camera is change of the bunch size with change of its excitation frequency. Result of this measurement is shown in Fig. 8. For this plot the frequency was changed once every second in 0.05 kHz steps. With image processing rate of 10 images per second it delivers ten data points per frequency. In case of the bunch size the obtained ten values were averaged to give one data point per frequency. However in case of center of mass motion the difference between maximal and minimal position is con-

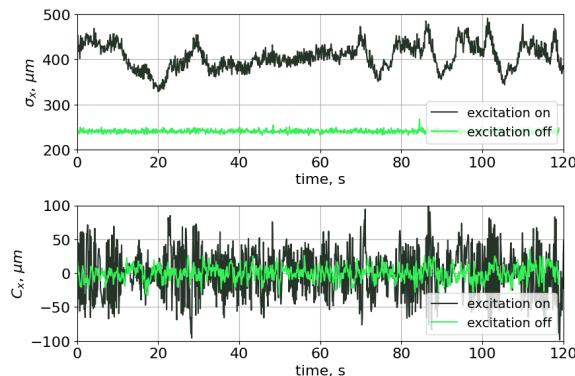


Figure 7: Change of the size and center of mass position for excited and not excited PPRE bunch.

sidered. The most important result of this test measurement is that at the currently chosen excitation frequency for standard user operation (f_{PPRE} on the plot) the ratio between bunch size and its motion is the highest as it is supposed to be. It can also be seen, that excitation at the betatron frequency (f_x) causes large motion of the bunch, without any significant increase of the bunch size.

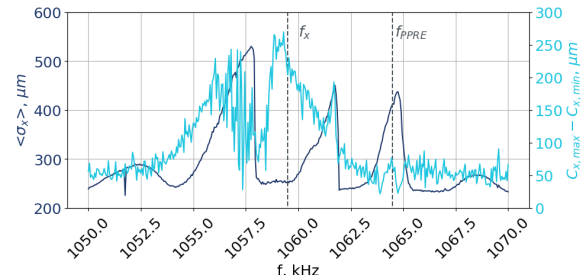


Figure 8: Change of the size and amplitude of center of mass position for different excitation frequencies of PPRE bunch.

So far only horizontal size of the bunch was of interest. In case of the vertical direction, it is important to note that due to the X-ray blocking baffle interference pattern in vertical direction appears. This effect can be seen in the Fig. 6 and can disturb analysis of the bunches in vertical direction.

CONCLUSION

The beamline for bunch resolved transverse optical diagnostics with combination of fast-gated ICCD camera is ready to be used for diagnostic purposes in the direct imaging mode. Transverse profiles of the individual bunches were successfully observed with the described set-up. Furthermore, first detailed observations of the PPRE bunch have been done, which showed the expected behaviour under conditions previously chosen for user operation. However this provides a new possibility of deeper understanding of the bunch excitation mechanism.

As any diagnostic tool, the fast-gated ICCD camera has its limitations. The most important ones are the image processing rate and limitation of spatial resolution by the MCP. Also for the direct imaging the resolution limit of the beamline has to be considered. However, interferometric method provides great solution to the limited resolution of the beamline. Implementation of this method in combination with the fast-gated ICCD is still ongoing.

REFERENCES

- [1] K. Holldack *et al.*, "Single bunch x-ray pulses on demand from a multi-bunch synchrotron radiation source", *Nat. Commun.*, vol. 5, no. 1, p. 4010, 2014. doi:10.1038/ncomms5010
- [2] J.-G. Hwang, M. Koopmans, M. Ries, A. Schaelicke and R. Mueller, "Analytical and numerical analysis of longitudinally coupled transverse dynamics of pulse picking by resonant excitation in storage rings serving timing and high-flux users simultaneously", *Nucl. Instrum. Methods Phys. Res., Sect. A*, vol. 940, pp. 387–392, 2019. doi:10.1016/j.nima.2019.06.053

[3] G. Schiawietz, J.-G. Hwang, A. Jankowiak, M. Koopmans and M. Ries, "Bunch-resolved diagnostics for a future electron-storage ring", *Nucl. Instrum. Methods Phys. Res., Sect. A*, vol. 990, p. 164992, 2021.
doi:10.1016/j.nima.2020.164992

[4] M. Koopmans, "Two-Dimensional Bunch-Resolved Optical Beam Diagnostics at BESSY II", Ph.D. dissertation, Phys. Dept., Humboldt-Universität zu Berlin, Berlin, Germany, 2022.
doi:10.18452/24232

[5] Stanford Computer Optics, <https://stanfordcomputeroptics.com/products/picosecond-iccd.html>

[6] G. Schiawietz *et al.*, "Approaching an optimum time resolution for synchroscan streak-camera measurements with visible synchrotron light", *Nucl. Instrum. Methods Phys. Res., Sect. A*, vol. 1062, p. 169196, 2024.
doi:10.1016/j.nima.2024.169196

[7] Dimtel, <https://www.dimtel.com/>